

Influence of Skin Type and Light Scattering on Induced Skin Temperatures during Nd:YAG and Alexandrite Laser Treatments in Dermatology

Jure Kosir,^{1,2} Rahul Sharma,² Matjaz Lukac^{2,3,4}

¹University of Ljubljana, Faculty for Mechanical Engineering, Ljubljana, Slovenia

²Fotona d.o.o., Stegne 7, Ljubljana, Slovenia

³Institut Josef Stefan, Light and Matter Dept., Jamova 39, Ljubljana, Slovenia

⁴University of Ljubljana, Faculty of Mathematics and Physics, Jadranska 19, Ljubljana, Slovenia

ABSTRACT

As a laser beam propagates into the skin, the effect of light scattering spreads the beam radially outward on each side, which decreases the beam's effective fluence. For this reason, a generally accepted paradigm in laser hair removal is to use larger laser spots, for which the effect of light scattering is expected to be smaller. In this paper, we report on a thermal imaging study on the influence of beam scattering when determining the appropriate Nd:YAG (1064 nm) and Alexandrite (755 nm) laser treatment fluences for different laser beam spot sizes and Fitzpatrick skin types.

Skin surface temperatures following pulsed laser irradiation were measured for different laser spot sizes and skin types. For the same incoming laser beam fluence, the skin surface temperature was observed to increase with the laser spot size. This dependence was found to be in good agreement with a model that assumes a spreading of the laser beam due to scattering by the same absolute amount of about 1.8 mm in diameter, independently of the size of the incoming beam diameter.

Key words: laser hair removal; Alexandrite laser, beam scattering, Nd:YAG laser, thermal imaging, Fitzpatrick skin types.

Article: J. LA&HA, Vol. 2023, No.1; preprint.

Received: July 19, 2023

© Laser and Health Academy. All rights reserved.

Printed in Europe. www.laserandhealth.com

I. INTRODUCTION

Laser hair removal has in recent years received wide clinical acceptance in both medical and aesthetics settings, because of its long-term results, non-invasive nature, minimal treatment discomfort, and the speed and ease with which procedures can be performed [1-4]. Commercial laser and flashlamp light (IPL) systems

differ by wavelength, pulse duration, fluence, laser beam delivery system and skin cooling method; all of which have an effect on the outcome of the treatment [5-16]. When deciding on the most appropriate light source for laser hair-removal treatments, their tissue interactions should be thoroughly analyzed and taken into consideration. Long-pulsed Alexandrite (755 nm) and Nd:YAG (1064 nm) solid crystal lasers have become preferred wavelengths for hair removal due to their effective absorption in the hair, and at the same time sufficient penetration to the deeply located hair roots within the skin [6]. In addition, as compared to other devices, it is only these two types of light sources that can deliver sufficiently high pulse powers at sufficiently short pulse durations (in a range of milliseconds) required for effective selective thermolysis of the hair within the surrounding skin matrix.

The absorption of the Alexandrite laser's wavelength in melanin is higher than that of Nd:YAG. This makes it more suitable for thermally damaging the melanin-rich hair. However, Nd:YAG with its weaker absorption in epidermal melanin, is safer for the treatment of darker skin types as it minimizes the risk of epidermal injury and pigmentary alteration. Therefore, a device containing both laser sources represents an optimal hair removal combination allowing safe and effective hair removal for all skin types.

Achieving satisfactory results when using a laser to treat unwanted hair depends on many factors. It has been demonstrated that successful permanent hair removal can only be achieved by injuring the bulb, the bulge and the outer root sheath of the hair follicle [1]. Therefore, the region in which these structures lie is the target for any method used to create the required injury to permanently remove the hair. During the process of laser hair removal, light is absorbed by chromophores (usually melanin in the hair shaft and follicle) and transformed into heat energy, resulting in a rise of the hair temperature. When the temperature is high enough, irreversible damage may occur to the hair structures, thus preventing or altering the growth of the hair.

Success is determined by tissue physics, hair physiology and the laser wavelength used in the treatment. An optimal laser fluence (i.e., laser pulse energy per irradiated area, in J/cm²) is the fluence that does not cause epidermal injury, yet remains sufficiently high for thermally damaging the hair after traversing the epidermis and reaching the deeply lying target. Therefore, to be able to select an appropriate fluence one must, among other factors, understand how the incident fluence is attenuated by the scattering of laser light within the skin matrix. Namely, as a beam propagates into the skin, light scattering spreads the beam radially outward on each side, which decreases the beam's effective fluence as it penetrates into the skin [17-21]. The influence of light scattering on the effective laser fluence has been studied for Nd:YAG (1064 nm) by numerical modeling and skin temperature measurements [20], however, similar measurements for the Alexandrite wavelength are lacking.

Another important factor when considering optimal hair removal laser fluences is the skin type. The most commonly used scheme to classify skin type according to a person's response to sun exposure in terms of burning and tanning was created in 1975 by Thomas B. Fitzpatrick [22, 23]. Laser hair removal is generally more effective and safer for lighter skin with dark hair than darker skin with dark hair because the epidermal melanin competes as a significant chromophore and may lead to excessive heating of the surrounding tissue, which may result in adverse effects such as epidermal blistering, hypopigmentation and scarring [6-9].

It is to be noted that the characteristics of laser light absorption and scattering in human skin play an equally important role in all dermatological procedures, and not just in hair removal. This is because most of dermatological and aesthetic laser treatments are based on thermally modifying or stimulating the treated tissue in a controlled manner. This involves either heating the tissue to temperatures below the critical temperature of tissue damage for non-ablative protocols, or removing tissue, lesions, vessels and other imperfections with the least possible residual heat deposition in more aggressive protocols.

In this paper, we report on a systematic thermal imaging study of the influence of beam scattering and skin type with respect to induced skin temperatures during dermatological treatments using Alexandrite (755 nm) and Nd:YAG (1064 nm) laser.

II. MATERIALS AND METHODS

The lasers used in this study (see Fig. 1), were the SP Dynamis[®], TimeWalker[®], and AvalancheLase[®]

systems (all manufactured by Fotona d.o.o.). All three systems are based on a dual-wavelength structure, with the SP Dynamis and TimeWalker including Er:YAG and Nd:YAG sources, and the AvalancheLase consisting of Alexandrite and Nd:YAG laser sources.

The lasers were equipped with the following non-contact handpieces (all manufactured by Fotona d.o.o.), with top-hat beam profiles at different selectable laser spot sizes (d) in a range from 2-30 mm: R33 (Nd:YAG; $d = 2-10$ mm), R34 (Nd:YAG; $d = 15$ and 20 mm), and R35 (Nd:YAG and Alexandrite; $d = 2-30$ mm).

The following calibrated measurement devices were used: a Quasar/PE50BF-DIF laser energy meter (manufactured by Ophir Optronics Solutions Ltd), a Molecron EM500/J50 laser energy meter (manufactured by Coherent Molecron Ltd), a DS4034 Ultra Vision digital oscilloscope (manufactured by Rigol Technologies, GmbH), a Matis thermal imager (manufactured by SAGEM, France), a FLIR A6750 SLS high-speed thermal camera (manufactured by FLIR Systems, USA); a ThermoCAM P45 thermal video camera (manufactured by FLIR Systems, USA); and a FAST M3K high-speed thermal camera (manufactured by Telops, Inc, Canada).



Fig. 1: Fotona SP Dynamis[®] (top left), TimeWalker[®] (top right), and AvalancheLase[®] (bottom) laser systems.

a) Neodymium:YAG laser modalities

The Nd:YAG laser operates at a wavelength of 1064 nm. Its most important characteristic is that it has very little affinity for water, which enables it to penetrate the skin for several millimeters, allowing it to reach and treat deeper structures [32]. Its predilection for blood and melanin are very useful to extend the range of applications that the Er:YAG laser cannot cover. This laser is available with a wide variety of selectable pulse durations (see Fig. 2), which extend from microseconds (FRAC3 mode) to milliseconds (VERSA mode) and seconds (PIANO® and PLLT modes), enabling it to produce different effects on its targets. One additional pulse option available for Nd:YAG only in the TimeWalker and Dynamis models is the Quasi Continuous Wave Mode (QCW), which, when delivered through a fine laser fiber, can be applied in surgical modalities such as laser lipolysis [33], endovenous laser ablation (EVLA) [34] and in the treatment of hyperhidrosis [35] or in skin subcision when treating valley scars [36].

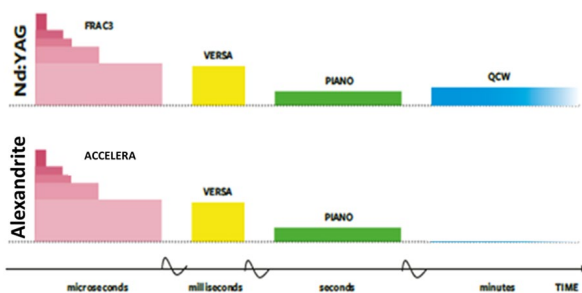


Fig. 2: The variety of pulse modalities available for the Nd:YAG and Alexandrite lasers in the SP Dynamis®, TimeWalker® and AvalancheLase® systems. The QCW mode is available only in the TimeWalker and Dynamis models.

b) Alexandrite laser modalities

The Alexandrite laser operates at a wavelength of 755 nm. Its most important characteristic is that it has a high affinity for melanin and a low affinity for water. Its higher predilection for melanin in comparison to Nd:YAG is very useful to complement the range of Nd:YAG applications. This laser is also available with a wide variety of selectable pulse durations (see Fig. 2), which extend from microseconds (ACCELERA mode) to milliseconds (VERSA mode) and seconds (PIANO® mode), enabling it to produce different effects on its targets.

c) Thermal imaging experiment

A thermal camera was fixed in position above the skin surface and focused on the treated skin site (Fig. 3). The laser beam was held at a fixed position and the maximal temperature increase $\Delta T = (T_{max} - T_{initial})$ was measured at the end of each laser pulse.

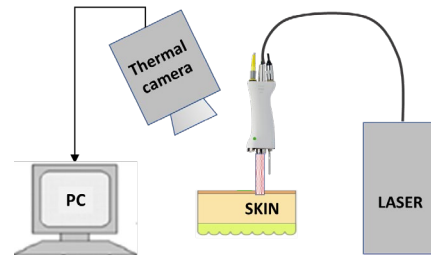


Fig. 3: Experimental set-up.

Measurements of the average skin surface temperature increase within the central part of the laser spot were performed in-vivo on skin of the dorsal hand area of each patient. No external or internal DMC™ (Dry Molecular Cooling) skin cooling was applied.

The measurements were made on Fitzpatrick II-V phototype patients [22, 23].

d) Dynamics of skin surface temperature evolution

The broad range of indications available with Nd:YAG and Alexandrite lasers cannot be attributed merely to their penetration depths and absorption characteristics, but equally well to the dual skin-heating dynamics of the temporal modalities available with these lasers (see Fig. 4).

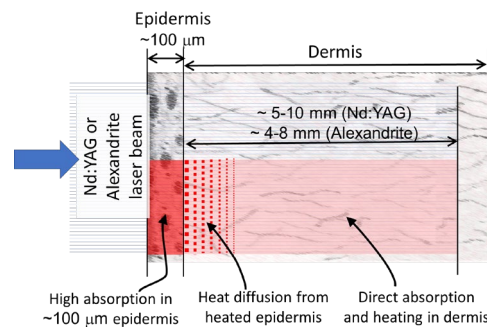


Fig. 4: Nd:YAG (1064 nm) and Alexandrite (755 nm) beam absorption and heat diffusion processes during a typical skin procedure. There are four major tissue-heating processes involved: a) Direct absorption of the laser light in the dermis within the penetration depth of $\sim 4-10$ mm; b) Selectively higher absorption of laser light within the melanin-rich, 100 μm thick epidermis; c) Fast heat diffusion from the highly heated epidermis to the underlying less heated dermis; d) Relatively slow cooling of the heated bulk tissue (epidermis and dermis) back to the initial temperature.

This is due to the fact that in spite of having different penetration depths, both lasers have relatively high partial absorption in the melanin-rich, appr. $d_{Nd,Alex} \approx 100 \mu\text{m}$ thick epidermis.

As a result of the absorption of the pulsed laser radiation, the temperature of the thin superficial layer, $d_{Nd,Alex}$ gets rapidly elevated. However, since this layer

is relatively thin, this temperature increase does not last long, due to the fast cooling provided by the rapid diffusion of the absorbed heat deeper into the less heated underlying skin layers.

The rate of cooling can be estimated by considering that the temperature of a heated tissue layer with a certain thickness d decays with an exponential decay (i.e., cooling) time $\tau \approx (1/D) d^2$, where $D \approx 0.11 \text{ mm}^2 \text{ s}^{-1}$ is the thermal diffusivity of the skin.

Based on the above approximate relation, the cooling time $\tau_{1-\text{Nd}}$ and $\tau_{1-\text{Alex}}$ of the $100 \text{ }\mu\text{m}$ thick epidermis can be estimated to be on the order of $\tau_{1-\text{Nd}}$, $\tau_{1-\text{Alex}} \approx 100 \text{ ms}$.

When considering the cooling rates of the underlying bulk tissue, these rates are significantly longer. In the case of the Nd:YAG or Alexandrite laser, the bulk tissue below the strongly heated superficial layer $d_{\text{Nd,Alex}}$ gets heated not only by the heat diffusion from the epidermis, but also predominantly and directly by the Nd:YAG's and Alexandrite's laser light penetrating through the epidermis, 4-10 mm deep into the dermis (see Fig. 4).

The corresponding estimated cooling times (τ_2) of the bulk tissues are therefore on the order of $\tau_{2-\text{Nd}}$, $\tau_{2-\text{Alex}} \approx 200\text{-}1000 \text{ s}$ for Nd:YAG and Alexandrite.

Based on the above, and depending on the duration (t_{laser}) of the laser irradiation, the superficial temperature dynamics during and following the Nd:YAG and Alexandrite laser irradiations follows one of the two temporal evolutions as shown in Fig. 5.

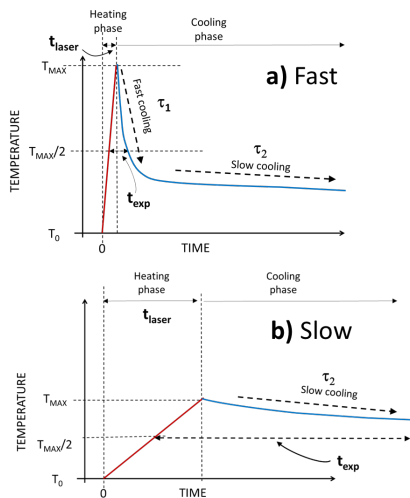


Fig. 5: Temporal evolution of the skin surface temperature during and following the Nd:YAG and Alexandrite laser irradiation for short (a-Fast) and long (b-Slow) laser pulse durations.

For laser pulse modalities with durations (t_{laser}) which are shorter than τ_1 , the skin surface temperature exhibits two decay characteristics, fast and slow, where the maximal temperature T_{max} initially decays with the fast-cooling time τ_1 , and then transitions into the slower cooling rate τ_2 of the bulk tissue. On the other hand, when t_{laser} is significantly longer than τ_1 , this gives the superficially heated layer sufficient time to continuously equalize its temperature with the underlying tissue, and therefore the skin surface temperature exhibits only a single, slow decay curve characterized by the bulk's slow-cooling time τ_2 .

A typical temporal evolution of the normalized skin temperature increase, $\Delta T/\Delta T_{\text{max}} = (T-T_0)/(T-T_{\text{max}})$ following a laser pulse is shown in Fig. 6. The temperature decay exhibited approximately two-exponential behavior, with the decay time τ_1 describing the decay behavior at short times, and the long decay time τ_2 describing the decay behavior at long times.

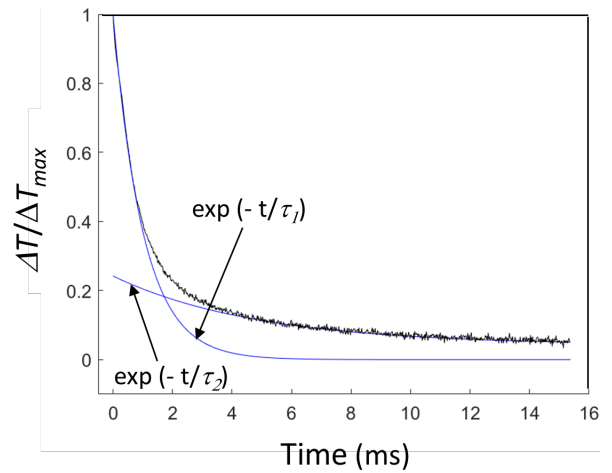


Fig. 6: Typical evolution of the normalized temperature increase $\Delta T/\Delta T_{\text{max}} = (T-T_0)/(T-T_{\text{max}})$ during the cooling phase [84]. The decay curve can be approximated by a superposition of two exponential curves, with τ_1 describing the decay behavior at short times and τ_2 describing the decay behavior at long times.

Very roughly, the exposure time t_{exp} , i.e., the duration of the tissue's exposure to T_{max} , can be approximated by taking FWHM (full width half maximum) durations of the thermal pulses: a) $t_{\text{exp}} \approx t_{\text{laser}}/2 + \tau_1 |\ln(0.5)|$, for "fast" laser irradiations; and b) $t_{\text{exp}} \approx t_{\text{laser}}/2 + \tau_2 |\ln(0.5)|$, for "slow" laser irradiations [27].

In what follows, the terms "FAST" and "SLOW" will be used for the following laser pulse modalities and durations, as shown in Table 1.

Table 1: Laser pulse duration modalities, as incorporated in Fotona Nd:YAG and Alexandrite laser systems.

Nd:YAG laser			
FAST		SLOW	
Mode	FRAC3	VERSA	PIANO & PLLT
t_{laser}	0.1-2 ms	3-25 ms	Seconds

Alexandrite laser			
FAST		SLOW	
Mode	ACCELERA	VERSA	PIANO
t_{laser}	0.1-2 ms	3-25 ms	Seconds

e) Heating coefficient

In this report, the induced tissue surface temperatures are quantified using a heating coefficient, $\eta = \Delta T / F$ (in $^{\circ}\text{C cm}^2 / \text{J}$), where ΔT (in $^{\circ}\text{C}$) = $T_{max} - T_0$ is the maximal temperature increase, and F (in cm^2 / J) = E_{laser} / S represents the laser pulse fluence, where E_{laser} (in J) is the laser pulse energy and S (in cm^2) is the laser spot size area. For a circular laser spot the laser spot size area is equal to $S = \pi d^2 / 4$, where d is the laser spot diameter.

f) Influence of laser spot size

As a beam propagates into the skin, light scattering spreads the beam radially outward on each side, which decreases the beam's effective fluence as it penetrates into the skin (see Fig. 7) [17, 19, 20].

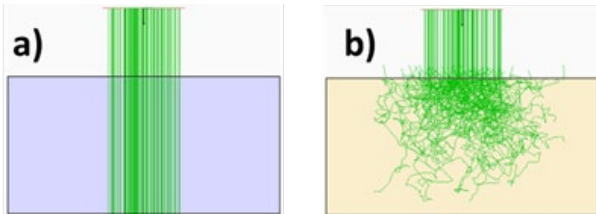


Fig. 7: Influence of scattering on beam propagation. a) In the absence of scattering, the beam remains focused and can penetrate deeper into the tissue; b) Due to scattering the beam spreads, and also gets reflected back to the melanin-rich epidermis where it may get absorbed. Figure presented with permission from [20].

An inexperienced laser system user may not immediately recognize the importance of the spot size of the incident beam as a treatment parameter. However, due to random laser light scattering, the spot size does make a difference to the treatment outcome [19]. This is because the effect of beam spreading is more pronounced for smaller spot sizes where the spreading of the beam is not negligible in comparison to the size of the incoming beam (see Fig. 8).

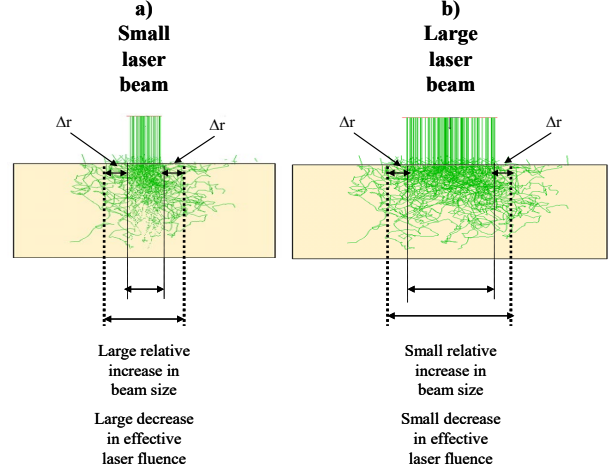


Fig. 8: Influence of scattering on the effective laser beam spot size (d'). The incident laser beam diameter d gets spread on both sides by Δr , resulting in an effective beam diameter $d' = d + 2\Delta r$. This effect is relatively less significant at larger spot sizes. Figure presented with permission from [20].

As a result of beam scattering, the incident laser beam diameter d gets spread on both sides by Δr , resulting in an increased effective beam diameter $d' = d + 2\Delta r$. Therefore, the incoming laser energy (E) initially contained in the incident beam spot area, $S = \pi d^2 / 4$, gets spread over a larger effective spot size area, $S' = \pi d'^2 / 4$. Accordingly, the incident fluence $F = E_{laser} / S$ gets reduced to the effective fluence $F' = E_{laser} / S'$. It is this reduced effective fluence that the skin is exposed to, resulting in a lower ΔT , and therefore in a lower heating coefficient, η' . Defining the maximal heating coefficient as $\eta_0 = \eta'(d = \infty)$, the heating coefficient at any spot size can then be expressed as $\eta'(d) = \rho(d) \times \eta_0$, where $\rho(d)$ is the scattering factor defining the reduction of the heating coefficient due to scattering. The spot size dependent effective fluence is then equal to $F'(d) = \rho(d) \times F$.

III. RESULTS

a) Influence of laser spot size for fast modalities

In what follows, it will be assumed that for a very large spot size of $d = 30$ mm, the scattering factor can be approximated by $\rho(d = 30 \text{ mm}) \approx \rho_0(d = \infty) = 1$. The measured dependence of the scattering factor ρ on the laser spot size diameter (d) for “fast” Nd:YAG and Alexandrite laser modalities and different Fitzpatrick skin types, is presented in Fig. 9.

As can be concluded from Fig. 9, the reduction of the heating coefficient due to beam scattering is approximately the same for both wavelengths, Nd:YAG and Alexandrite, and all tested skin types. Using the fit with $2\Delta r = 1.8$ mm, and defining $\rho(d =$

30 mm) = 1, the approximate relative dependence of the heating reduction factor ρ on the spot size is presented in Table 3 below.

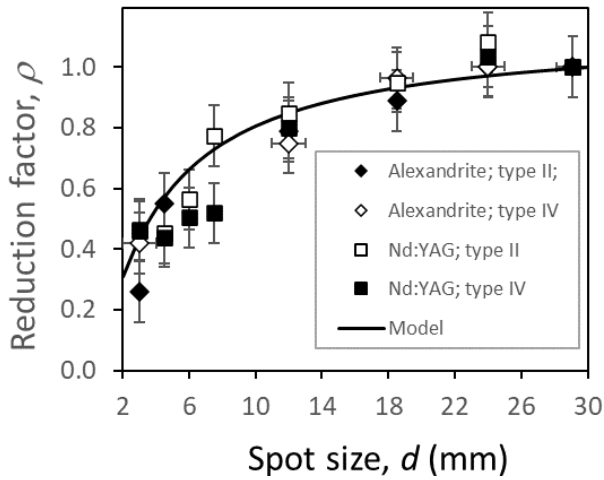


Fig. 9: Dependence of the measured scattering factor (ρ) on the incident laser beam spot size (d), for “fast” Nd:YAG and Alexandrite laser modalities, and Fitzpatrick skin types II and IV. The line represents a fit to the experimental data, assuming that the effective beam diameter $d' = d + 2\Delta r$ gets increased by the same distance, $2\Delta r = 1.8$ mm.

Table 3: Relative dependence of the scattering factor (ρ) on the laser spot diameter d , for the “fast” Nd:YAG and Alexandrite laser modalities.

d (mm)	2	3	4	5	6	10	15	20	25	30
ρ	0.31	0.44	0.53	0.61	0.66	0.81	0.90	0.95	0.98	1

b) Cooling times for FAST modalities

Figure 10 shows the measured temperature decay times following a “fast” 1 ms long Nd:YAG laser pulse for different Fitzpatrick skin types (Fig. 10).

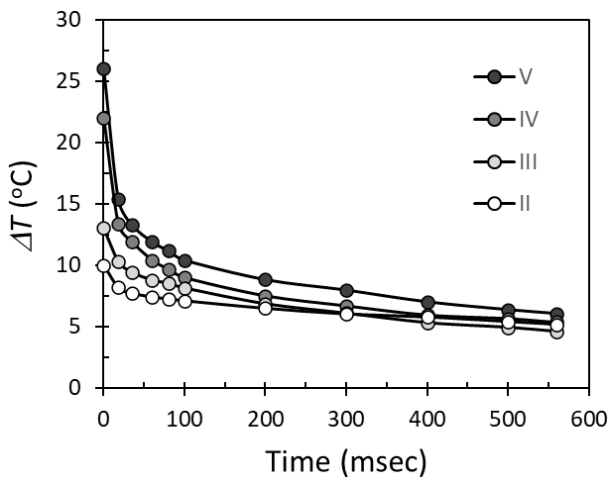


Fig. 10: Skin surface temperature decay curves following a 1 ms Nd:YAG laser pulse duration, $d = 4$ mm spot size, $F = 30$ J/cm², for Fitzpatrick skin types II-V.

The corresponding normalized temperature decay curves, and temperature decay times τ_i are shown in Fig. 11 and Table 4.

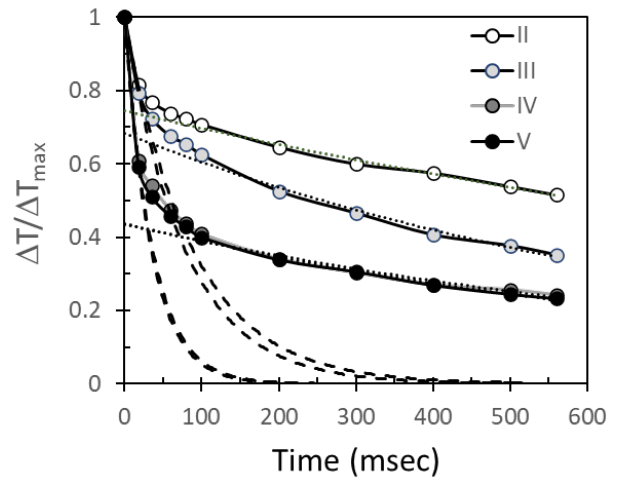


Fig. 11: Normalized skin surface temperature decay curves from Fig. 12. The dashed lines represent fits to the initial fast decaying segments of the curves (τ_i), and the dotted lines represent fits to the subsequent slower decaying segments of the curves.

Table 4: Fast decay times for fast Nd:YAG irradiations, for different Fitzpatrick times. The decay times for the Alexandrite laser, characterized by a higher absorption in melanin, are on the order of 35 msec for all skin types.

	II	III	IV	V
τ_1 (msec)	88.5	89.3	36.2	34.4

The estimated thermal exposure times (t_{exp}) for Nd:YAG and Alexandrite lasers are shown in Table 5.

Table 5: Estimated thermal exposure times (t_{exp}) for fast Nd:YAG and Alexandrite pulse modalities.

		II	III	IV	V
t_{exp} (ms)	Nd:YAG	65	65	30	30
	Alexandrite	30	30	30	30

c) Influence of laser pulse duration for FAST modalities

The dependence of the measured Nd:YAG laser heating coefficient ρ_0 ($d = 30$ mm) on the laser pulse duration and Fitzpatrick skin type is shown in Fig. 12.

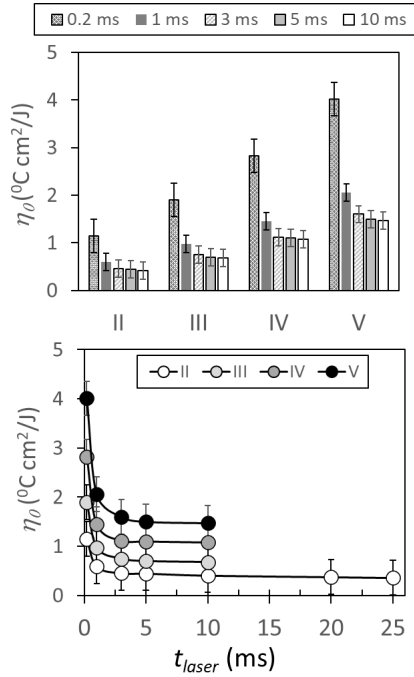


Fig. 12: Dependence of the measured Nd:YAG laser heating coefficient ρ_0 ($d = 30$ mm) on the laser pulse duration and Fitzpatrick skin type.

As can be seen from Fig. 12, the heating coefficient is slowly decreasing only for pulse durations $t_{laser} \geq 3$ ms, and starts to quickly increase for pulse durations $t_{laser} \leq 2$ ms.

In skin types where light is strongly absorbed within the epidermis, the absorbed heat is concentrated closer to the surface and the deeper-lying dermal skin layers are less heated. Since conduction is faster for larger temperature gradients, the darker skin types can cool more readily into the slightly cooler dermis below.

d) Heating coefficient for FAST modalities

Measured heating coefficients η_0 ($d = 30$ mm), for Nd:YAG and Alexandrite laser wavelengths for pulse durations $t_{laser} = 3$ -10 ms, are presented in Fig. 13.

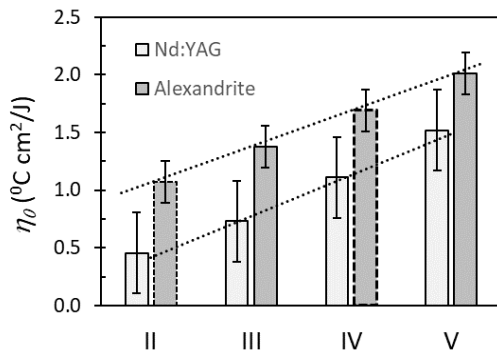


Fig. 13: Heating coefficients η_0 ($d = 30$ mm) for Nd:YAG and Alexandrite laser wavelengths for pulse durations $t_{laser} = 3$ ms.

The obtained heating coefficients η_0 for the Nd:YAG and Alexandrite lasers, for different laser pulse durations and Fitzpatrick skin types are shown in Table 6 below.

Table 6: Heating coefficients η_0 for different laser pulse durations and Fitzpatrick skin types, for Nd:YAG and Alexandrite laser.

		Nd:YAG laser					
		t_{laser}	II	III	IV	V	VI
FRAC3	0.2 ms	1.15	1.90	2.82	4.01	4.93	
	1 ms	0.59	0.98	1.45	2.06	2.53	
	2 ms	0.48	0.78	1.18	1.63	2.00	
VERSA	3 ms	0.45	0.73	1.11	1.52	1.87	
	4 ms	0.44	0.70	1.10	1.50	1.85	
	10 ms	0.41	0.68	1.06	1.41	1.74	
	15 ms	0.40	0.65	1.03	1.34	1.66	
	25 ms	0.36	0.48	0.76	0.99	1.23	

		Alexandrite laser				
		t_{laser}	II	III	IV	V
ACCELERA	0.2 ms	2.24	3.59	4.39	5.23	
	1 ms	1.15	1.79	2.20	2.61	
	2 ms	1.09	1.48	1.82	2.16	
VERSA	3 ms	1.07	1.38	1.69	2.01	
	4 ms	1.05	1.36	1.67	1.95	
	10 ms	1.04	1.30	1.61	1.88	
	15 ms	0.95	1.22	1.50	1.78	
	25 ms	0.70	0.90	1.11	1.32	

e) Differences between SLOW and FAST modalities

A schematic presentation of the difference in the temperature distribution within the skin for “fast” (VERSA modality) and “slow” (PIANO modality) pulse durations is shown in Fig. 14 [31, 37, 38].

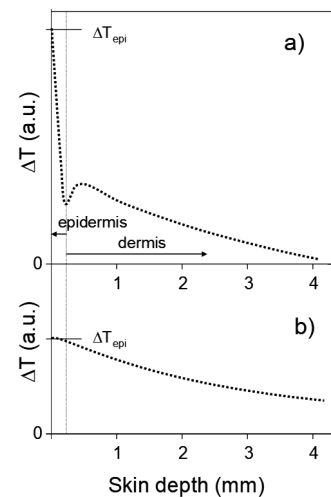


Fig. 14: Calculated temperature distribution immediately after a fast (VERSA mode) Nd:YAG laser pulse with $t_{laser} < \tau_t$ (a), and after a slow (PIANO mode) long duration Nd:YAG laser pulse with $t_{laser} \gg \tau_t$ (b). The figure is reprinted with permission from [37].

Figure 15 shows the measured temperature evolution on the hand skin following Nd:YAG laser radiation with a “slow” 1.5 s long PIANO pulse, and a “fast” 20 ms long VERSA pulse, for the same pulse fluence [39].

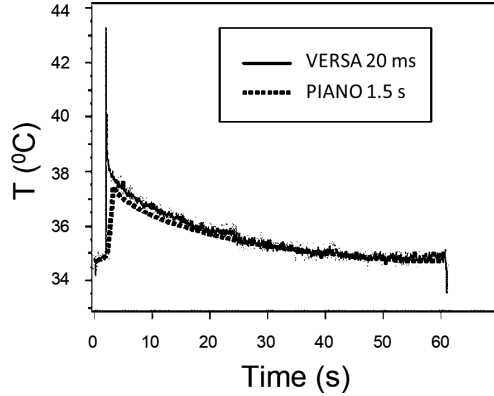


Fig. 15: Measured temperature evolution of dorsal hand skin following irradiation with the Nd:YAG laser PIANO (1.5 s) pulse mode, and VERSA (20 ms) pulse mode. The laser pulse fluence was the same for both pulse duration modes. The figure is reprinted with permission from [37].

As expected from Fig. 14, the measured peak epidermal temperature is higher with the fast 20 ms long Nd:YAG laser pulse. After approximately 0.5 s when the epidermal temperature gets equalized with the temperature of the lower lying dermis, the surface skin temperature has approximately the same temperature decay dependence, regardless of the Nd:YAG pulse duration. This demonstrates that with the PIANO mode, the same temperatures of the bulk dermis are achieved as with shorter pulse durations. However, with the PIANO mode, high initial temperature peaks in the epidermis are completely avoided.

It is also important to note that with the long duration (SLOW) modalities, the heating coefficients and the cooling times are the same for both the Nd:YAG and Alexandrite laser wavelengths. They are also predominantly independent of the Fitzpatrick skin type. This is because during the SLOW irradiations, the heated epidermis has sufficient time to continuously equalize its temperature with the underlying dermis, which essentially removes the influence of the differences in laser absorption in the epidermis. As an example, Fig. 16 shows the measured skin surface temperature evolution following irradiations by Nd:YAG or Alexandrite PIANO pulses of the same duration and fluence, with $t_{laser} = 30$ s and $F = 24$ J/cm².

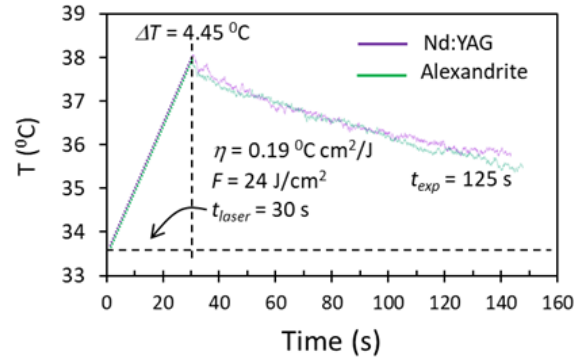


Fig. 16: Comparison of the measured skin temperature evolutions following irradiation with the Nd:YAG or Alexandrite laser PIANO ($t_{laser} = 30$ s) pulse mode, with the same fluence of $F = 24$ J/cm². Both irradiations result in the same $\Delta T_{max} = 4.45$ °C, and essentially the same temperature decay behavior.

Additionally, the influence of the laser spot size on the heating coefficient (η) is different for the “slow” pulse modality in comparison to that of the “fast” modality, as presented in Fig. 9 and Table 3. This is because during slow (long duration) modalities, the heat diffusion in the radial direction becomes appreciable as well, in addition to the beam scattering in the radial direction. For this reason, the increase in the heating coefficient does not saturate at $d \approx 30$ mm (see Fig. 9) but was measured to continue increasing for spot sizes up to $d \approx 90$ mm, and is projected to continue higher (see Fig. 17).

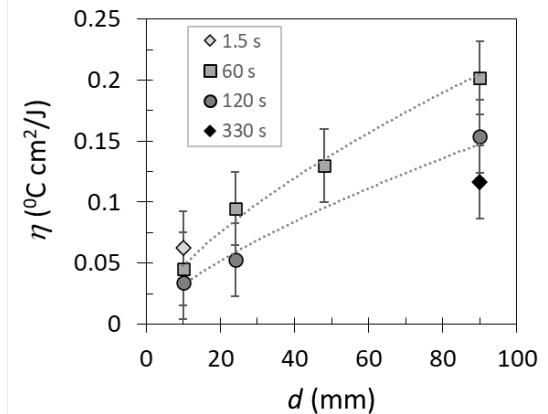


Fig. 17: Measured dependence of the heating coefficient on the laser spot size for the “slow” (PIANO) Nd:YAG modality. The data for $d = 90$ mm is obtained from measurements using a Fotona L-Runner scanner irradiating a skin area of 8×8 cm² [38].

f) Heating coefficient for SLOW modalities

The measured heating coefficients η for Nd:YAG and Alexandrite laser wavelengths, and for different laser spot sizes, as a function of the PIANO pulse duration, are presented in Fig. 18.

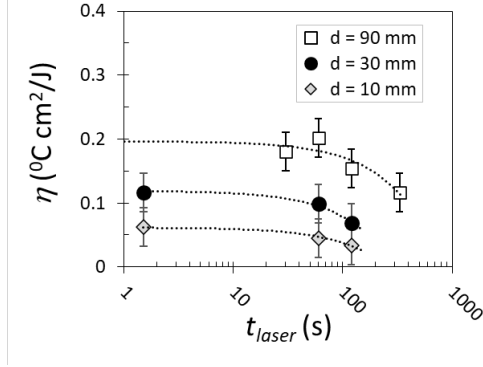


Fig. 18: Dependence of the heating coefficient η on the “slow” (PIANO mode) pulse duration for Nd:YAG and Alexandrite laser wavelength, and for different laser spot sizes.

IV. DISCUSSION

The thermal imaging test results demonstrate that the range of laser output modalities available in the Fotona devices incorporating Nd:YAG and Alexandrite laser technology (Fig. 2 and Table 1) provides practitioners with the capability to adjust the treated tissue’s temperature and thermal exposure time depending on the treated indication.

It is important to note that it is not only the amplitude of the tissue’s temperature elevation which determines the extent of any thermal damage, but also (and of equal importance) the duration of the elevated temperature. The importance of the difference in the cooling times for the three laser wavelengths and their pulse modalities can be best appreciated by considering that the thermal damage kinetics during laser procedures is commonly described by the Arrhenius damage integral [29], and that according to the Arrhenius’ model the critical temperature (T_{crit}) for irreversible tissue damage is higher for short thermal exposures (t_{exp}) and increases significantly for extremely short duration exposures [29].

A commonly used metric for tissue damage (Ω) is the ratio of the concentration of (undamaged) tissue before thermal exposure (C_0) to the concentration of native tissue at the end of the exposure time (C_f). The tissue damage is then calculated using the Arrhenius damage integral calculated over the time of the thermal exposure [29]:

$$\Omega = \ln (C_0/C_f) = A \int \exp(-E/RT(t)) dt . \quad (1)$$

Here, A is the frequency factor, i.e. the damage rate (in s^{-1}), E is the activation energy [in J/kmol], and R is the gas constant ($R= 8.31 \cdot 10^3$ J/kmol K).

The tissue damage kinetics is then commonly characterized by a critical (i.e., damage threshold)

temperature (T_{crit}) which is, assuming a square-shaped temperature pulse with a constant temperature during the thermal exposure time (t_{exp}), defined by [31]:

$$T_{crit} = E / (R \ln(A t_{exp})) \quad (2)$$

and represents the temperature at which the concentration of the undamaged tissue is reduced by a factor of e (i.e., when $\Omega = 1$).

Studies of tissue damage dynamics demonstrate that when considering extremely short and long exposure times, cell viability cannot be described by a single biochemical process [30]. For example, measurements of damage threshold temperatures at extremely short exposure times (commonly present during Er:YAG laser treatments) exhibit a shift to temperatures which are much higher than what would be expected from a single biochemical process characterizing the damage dynamics at long exposure times [24–28].

Figure 19 shows the published measured critical temperatures in soft human tissue for different exposure times [24–29], together with the VHS (Variable Heat Shock) model [30], which describes the dependence of T_{crit} on t_{exp} by assuming that the cell viability can be described as a combined effect of two biochemical processes that dominate cell survival characteristics at very short and very long exposure times.

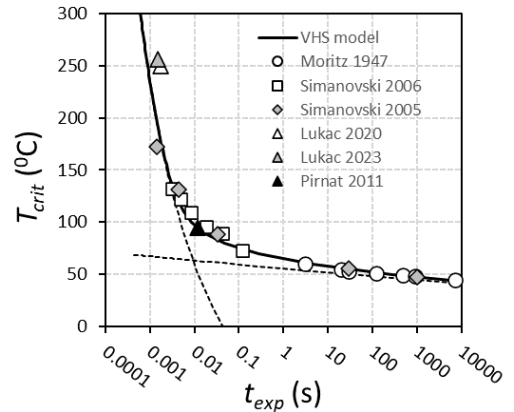


Fig. 19: Dependence of the published measured critical (damage threshold) temperatures T_{crit} on the duration of thermal exposure t_{exp} [29, 24, 25, 26, 27, 28], together with the critical temperature curve according to the VHS model [27, 30], representing the combined effect of two limiting biochemical processes that define cell viability at extremely long and extremely short exposure times.

Therefore, when evaluating an acceptable maximal tissue temperature during a specific laser procedure, it is important to take into account the thermal exposure time, t_{exp} (see Table 5).

V. CONCLUSIONS

In summary, the combination of Nd:YAG and Alexandrite laser technology can be applied to a vast spectrum of medical protocols that are present in the clinician's everyday practice, being capable of covering treatments to the epidermis, dermis, mucosa, subcutaneous tissue and fat by using the available set of laser wavelengths and pulse modalities, and of the corresponding tissue's thermal exposure times.

ACKNOWLEDGMENT

This study was partially financed by the Slovenian Research Agency ARIS under grant P1-0389 (MedFiz-Medical Physics).

REFERENCES

1. Goldberg D.J., Laser hair removal, Martin Dunitz, 2000.
2. Landthaler M et al, Effects of argon, dye and Nd:YAG lasers on epidermis, dermis and venous vessels, *Lasers Surg Med* 1986, 6:87-93.
3. Wanner M., Laser hair removal, *Dermat. Therapy*, 2005, Vol.18, 209-216.
4. Olsen EA. Methods of hair removal. *J. Am Acad dermatol.*; 1999,40:143-55.
5. I. Galadari, 'Comparative evaluation of different hair removal lasers in skin types IV, V, and VI', *Int J Dermatol*, vol. 42, no. 1, pp. 68–70, Jan. 2003, doi: 10.1046/j.1365-4362.2003.01744.x.
6. A. Krasniqi, D. P. McClurga, K. J. Gillespiea, and S. Rajpara (2022) Efficacy of lasers and light sources in long-term hair reduction: a systematic review. *J Cosmet Laser Therapy*. 2022, 24/1–5: 1–8.
7. M. Lukac, L. Grad, Scanner Optimized Aesthetic Treatments with the VSP Nd:YAG Lasers, *J. Cosmetic Laser Therapy*, Vol. 10, No.2, June 2008.
8. M. Lukac, L. Grad, K. Nemeš, Scanner Optimized Efficacy (SOE) Hair Removal with the VSP Nd:YAG Lasers, *J. of Laser and Health Academy*, Vol. 2007/1, No.3; www.laserandhealth.com.
9. L. Grad, T. Sult, R. Sult, Scientific Evaluation of the VSP Nd:YAG Laser for Hair Removal, *J. Laser and Health Academy*, Vol. 2007/1, No.2, www.laserandhealth.com.
10. Raff K., Landthaler M., Hohenleutner U., Optimizing treatment for hair removal using long-pulsed Nd:YAG lasers, *Lasers in Med.Sci.*, 2004,18:219-222.
11. Goldberg D.J., Silapunt S., Hair removal using a long pulsed Nd:YAG laser: Comparison at fluences of 50, 80 and 100 J/cm², *Dermatol Surg* 2001, 27: 434-436.
12. Tanzi E.L., Alster T.S., Long Pulsed 1064 nm Nd:YAG laser assisted hair removal in all skin types, *Dermato.Surg.*, 2004,30:13-17.
13. Battle E, Hobbs L.M., Laser assisted hair removal for darker skin types, *Derm. Therapy*, 17, 2004, 177-183.
14. Bencini P.L et al, Long term epilation with long pulsed neodymium:YAG laser, *Dermatol.Surg.*, 25:3, 175:178.
15. Ferraro G.A et al, Neodymium Yttrium Aluminum garnet long impulse laser for the elimination of superfluous hair: Experiences and considerations from 3 years of activity, *Aesth.Plast.Surg.*, 2004, 28:431-434.
16. Rogachefsky A.S., D.J.Goldberg, et al, Evaluation of a long pulsed Nd:YAG laser at different parameters: An analysis of both fluence and pulse duration, *Dermatol. Surg.*, 2002, 28:932-936.
17. Anderson R, Parrish J., The optics of human skin, *J Invest Dermatol.*; 1981,88:13-19.
18. B.C. Wilson and G. Adam. A Monte Carlo model of absorption and flux distributions of light in tissue. *Med. Phys.* 1983,10, 824-830.
19. Baumler W et al, The effect of different spot sizes on the efficacy of hair removal using a long-pulsed diode laser, *Dermatol Surg.*, 2002, 28(2):118-121.
20. M. Lukač, M. Gorjan, J. Žabkar, L. Grad, and Z. Vizintin, 'Beyond Customary Paradigm: FRAC3® Nd:YAG Laser Hair Removal', *LA&HA J. Laser and Health Academy*, vol. 2010/1, no. 1, pp. 35–46, 2010.
21. Shimojo Y, Nishimura T, Hazama H, Ito H, Awazu K (2021) Incident Fluence Analysis for 755-nm Picosecond Laser Treatment of Pigmented Skin Lesions Based on Threshold Fluences for Melanosome Disruption. *Lasers Surg Med.* 2021, 53(8): 1096–1104.
22. Fitzpatrick TB (1988) The validity and practicality of sun-reactive skin types I through VI. *Arch Dermatol* 124:869–871.
23. Pathak MA, Fitzpatrick TB (1993) Preventive treatment of sunburn, dermatoheliosis, and skin cancer with sun protective agents. In: Fitzpatrick TB, Eisen AZ, Wolff K et al (eds) *Dermatology in general medicine*, 4th edn. McGrawHill, Inc, New York, pp 1689–1717.
24. Simanovskii D. M., Mackanos M. A., Irani A. R., O'Connell-Rodwell C. E., Contag C. H., Schwettman H. A., and Palanker D. V., Cellular tolerance to pulsed hyperthermia, *Phys Rev E* 74, 011915 (2006), doi: 10.1103/PhysRevE.74.011915.
25. Simanovskii D., Sarkar M., Irani A., O'Connell-Rodwell C., Contag C., Schwettman A., Palanker D., Cellular tolerance to pulsed heating, *Proc. of SPIE* 5695, 254-259 (2005), doi: 10.1117/12.601774.
26. Lukac N., Tasic Muc B., Lukac M. "High-Temperature Triggering of Soft-Tissue Regeneration by Er:YAG Laser". *J LA&HA, J Lasers Health Acad* (2020) 2021/1:S3.
27. Lukač M., Košir J., Žel T., Kažič M., Šavli D., Jezeršek M. Influence of Tissue Desiccation on Critical Temperature for Thermal Damage during Er:YAG Laser Skin Treatments. *Lasers Surg Med.* (2023).
28. Pirnat S, Lukac M, Ihan A (2011) Thermal tolerance of E. faecalis to pulsed heating in the millisecond range. *Lasers Med Sci* (2011) 26:229–237.
29. Moritz AR, Henriques FC (1947) Studies of thermal injury, 2. The relative importance of time and surface temperature in the causation of burns. *A J Pathol* 23:695–720.
30. Lukac M, Lozar A, Perhavec T, Bajd F. "Variable heat shock response model for medical laser procedures", *Lasers Med Sci* (2019). <https://doi.org/10.1007/s10103-018-02704-1>.
31. Lukac, M, et al. "TightSculpting®: A Complete Minimally Invasive Body Contouring Solution; Part I: Sculpting with PIANO® technology." *J LA&HA- J Laser Health Acad* 2018.1 (2018): 16-25.
32. Yamagami, T., Handa, H., Takeuchi, J. et al. Extent of thermal penetration of Nd-YAG laser — histological considerations. *Neurosurg. Rev.* 7, 165–170 (1984).
33. Lukac M, Vizintin V., Zabkar J., Pirnat S. "QCW Pulsed Nd:YAG 1064 nm Laser Lipolysis". *J LA&HA, J Lasers Health Acad* Vol. 2009; No.4/1.
34. Šikovec, A. "Saphenous vein occlusion by endovenous laser ablation (EVLA) with a 1064 nm VSP Nd: YAG laser." *J LA&HA, J Lasers Health Acad* 2010.1 (2009): 19-23.
35. Goldman, A, and Wollina U. W. E.. "Subdermal Nd-YAG laser for axillary hyperhidrosis." *Dermatologic surgery* 34.6 (2008): 756-762.
36. Lipper, Graeme M., and Perez M. Nonablative acne scar reduction after a series of treatments with a short-pulsed 1,064-nm neodymium: YAG laser. *Dermatologic surgery* 32.8 (2006): 998-1006.
37. Lukac M, Vizintin Z, Pirnat S, Nemes K (2011) New Skin Treatment Possibilities with PIANO Mode on an Nd:YAG Laser. *J LA&HA, J. Laser and Health Academy*, vol. 2011/1, no. 1, pp. 22-32.
38. Lukac M, Levičnik Hoeffler S, Terlep S, Hreljac I, Vampelj U, Gorsic Krisper M, Vizintin Z (2022) Characteristics of Piano Level Laser Therapy (PLLT™) Using Novel 1064 nm Laser Handpiece Technology. *J LA&HA, J. Laser and Health Academy*, vol. 2022/1, no. 1, pp. 1-6.

The intent of this Laser and Health Academy publication is to facilitate an exchange of information on the views, research results, and clinical experiences within the medical laser community. The contents of this publication are the sole responsibility of the authors and may not in any circumstances be regarded as official product information by medical equipment manufacturers. When in doubt, please check with the manufacturers about whether a specific product or application has been approved or cleared to be marketed and sold in your country.